A&A 508, 707–716 (2009)
DOI: 10.1051/0004-6361/200912584


Astronomy & Astrophysics

# Characterising discs around Herbig Ae/Be stars through modelling of low-$J$ $^{12}$CO lines

O. Panić and M. R. Hogerheijde

Leiden Observatory, Leiden University, PO Box 9513, 2300 RA, Leiden, The Netherlands
e-mail: olja@strw.leidenuniv.nl

Received 27 May 2009 / Accepted 6 July 2009

**ABSTRACT**

*Context.* While there has been extensive investigation of the dust emission in discs around young intermediate-mass or Herbig Ae/Be stars at a range of wavelengths, their gas content has been systematically studied mainly via spatially unresolved (sub)millimetre observations of the rotational lines of $^{12}$CO.
*Aims.* We are interested in how the available low-$J$ $^{12}$CO spectra compare to the disc properties inferred from the dust emission, and to what extent the gas- and dust-emission approaches to disc modelling are complementary to each other.
*Methods.* First, we use the disc structure derived from the spectral energy distribution (SED) modelling to produce the synthetic $^{12}$CO $J = 3-2$ spectra for a discrete sample of sources. We then compare these synthetic spectra to observations, to test the existing disc models for each source. In our second approach, we study the dependence of the $^{12}$CO $J = 3-2$ spectrum on disc size, inclination and temperature, for discs around Herbig Ae/Be stars in general. We calculate the spectral line profiles for a grid of parametric disc models. The calculated spectra are compared to the spectra observed towards a large sample of sources. Both methods use a molecular excitation and radiative transfer code for the calculation of the $^{12}$CO line emission.
*Results.* SED models are insensitive to the parameters that dominate the low-$J$ $^{12}$CO emission, i.e., the disc size and orientation. To minimise some of the important parameter degeneracies, it is necessary to model a disc's SED with prior knowledge of the disc size and inclination. We show how the spectral profile of low-$J$ $^{12}$CO lines can be used to constrain these parameters, and to obtain disc models that are good starting points for the *outside-in* SED modelling of discs from long to shorter wavelengths.
*Conclusions.* For a disc gas mass of the order of 0.01 $M_\odot$, the optically thick $J = 3-2$ $^{12}$CO line intensity shows that the majority of discs around Herbig Ae/Be stars are smaller than 200 AU, and that the largest and brightest sources thoroughly studied with submillimetre interferometry are not representative of the sample.

**Key words.** planetary systems: protoplanetary disks – stars: pre-main-sequence

## 1. Introduction

The physical processes that shape circumstellar discs during their evolution ultimately determine the amount of material available for, and the timescale of the planet formation. The dust grain growth and settling to the disc midplane are probed by mid-infrared spectroscopy (Bouwman et al. 2001; van Boekel et al. 2003) and the spectral energy distribution (SED) from the near-infrared to millimetre wavelengths (Dullemond & Dominik 2004, 2005). Disc modelling based on both SED and the mid-infrared spectrum has thus developed, and this approach has been combined with near-infrared and millimetre imaging and/or interferometry (Pinte et al. 2008; Tannirkulam et al. 2008). However, the dust presents only a small percentage of the disc mass contained in molecular gas. Accretion, photoevaporation and photodissociation disperse the gas reservoir, and limit the timescale for gaseous planets to form. Due to these mechanisms, the mass ratio between the gas and the dust is expected to decrease with time, as the disc structure dominated by the gas pressure gradients and rotation becomes flatter and gas and dust decoupled. The bulk of the disc gas is best traced via submillimeter emission lines of abundant molecular species like $^{12}$CO and its isotopologues ($^{13}$CO, C$^{17}$O, C$^{18}$O) (Guilloteau & Dutrey 1994; Mannings & Sargent 1997; Thi et al. 2001; Dent et al. 2005). However, the main problem in determining the gas mass is the uncertainty in the gas phase abundance of $^{12}$CO, as this molecule is efficiently frozen onto dust grains at the low temperatures. Temperatures lower than 20 K are common in the dense midplane of discs around pre-main-sequence stars of spectral type M and K, and stellar mass $<1$ $M_\odot$ (T Tauri stars). The intermediate-mass pre-main-sequence stars, referred to as Herbig Ae/Be stars, are surrounded by discs of gas and dust observationally similar to those around T Tauri stars (Mannings & Sargent 1997, 2000; Natta et al. 2000). Due to the spectral type F to B of their central stars, these discs are warmer and provide an opportunity to overcome the uncertainty in the CO gas phase abundance, rendering CO a more reliable tracer of the entire disc. Motivated by the recent estimate of the gas-to-dust mass ratio (Panić et al. 2008) in a 200 AU disc around an A type star HD 169142 unaffected by freeze-out, we further explore the known gas-rich discs around Herbig Ae/Be stars. We aim to identify other sufficiently small and warm discs 'immune' to CO freeze-out, and establish whether these are statistically representative of the sample of known gas-rich discs around Herbig Ae/Be stars.

Our comparative study of the gas and dust content of discs focuses on a sample of nine Herbig Ae/Be stars, listed in Table 1, towards which the $^{12}$CO $J = 3-2$ line is firmly detected and associated with a circumstellar disc (Dent et al. 2005; Thi et al. 2001, 2004). The sources range from those with relatively weak $^{12}$CO $J = 3-2$ line emission, to some of the brightest and known

sources like HD 163296 and AB Aur (Isella et al. 2007; Piétu et al. 2005; Schreyer et al. 2008). The spectral type spans from late F to late B. Our choice of these sources was guided by the availability of SED models of the disc physical stucture from Dominik et al. (2003). In our study of the $^{12}$CO $J = 3-2$ line emission from discs around Herbig Ae/Be stars in general, we use our observations of HD 100546 and the data for 21 sources from Dent et al. (2005) in which this line was detected ($>2\sigma$). Dent et al. (2005) carried out the largest search for gas in discs around young Herbig Ae/Be stars so far. Their full target list of 59 young stars includes the Malfait et al. (1998) sample of isolated Herbig Ae/Be stars with IR excess due to circumstellar dust. The 21 sources we use here are a subset biased towards the sources with stronger $^{12}$CO emission. Any discs with low amounts of gas that may have been missed in this way do not affect the conclusions of our study.

We investigate the physical disc properties, primarily the size and temperature, that can be constrained by the $^{12}$CO low-$J$ spectral line profiles, as well as the disc inclination, as an important parameter in disc modelling. Single dish observations of the $^{12}$CO $J = 3-2$ line from the literature are complemented with our JCMT $^{12}$CO $J = 2-1$ line observations presented in Sect. 2. The $^{12}$CO $J = 3-2$ observations are used in Sect. 3 to test the structure proposed by the existing SED-based disc models for nine Herbig Ae/Be stars. A molecular excitation and radiative transfer code was used to calculate the emission from the disc model structure, which is then compared to the observations. We find that the SED modelling without a prior knowledge of disc size and inclination tends to produce models that are incompatible with the observed submillimetre line emission, often underestimating the disc size. In Sect. 4 we calculate the $^{12}$CO $J = 3-2$ emission using a grid of simple parametric disc models, with disc size and inclination as free parameters. We find that our model results predict the observed spread in integrated intensity and line-width, as well as the lack of strong and wide lines in a larger sample of Herbig Ae/Be discs. Although the number of known discs with weak low-$J$ $^{12}$CO lines is limited by the sensitivity of the instruments, the small discs (<200 AU) are clearly more frequent than the large ones. We discuss the implications of our parametric models for the particular sources in our sample, and find that the results of our simple models compare well to the size and inclination measured by the interferometric submillimeter, near-infrared and/or mid-infrared observations already available for some of these sources. Section 5 summarises our results and conclusions and outlines the future prospects.

## 2. Observations and results

We observed the $^{12}$CO $J = 2-1$ line toward the sources HD 135344, HD 179218, HD 142666, HD 139614 and V892 Tau using the James Clerk Maxwell Telescope (JCMT) and the $^{12}$CO $J = 3-2$ line toward HD 100546 using the Atacama Pathfinder Experiment (APEX) telescope[1].

The observations of the $^{12}$CO $J = 2-1$ line, at the rest frequency of 230.538 GHz, were carried out using the heterodyne receiver RxA3 on the JCMT. The JCMT beam size at 230 GHz is 21″ and beam efficiency 0.9. The integration times were approximately 20–30 min on-source. The data were obtained in 2008 September under good weather conditions, with the atmospheric opacity $\tau_{230\ \mathrm{GHz}} \approx 0.2$. Figure 1 shows the JCMT observations towards the remaining four sources. The rms level of the $^{12}$CO $J = 2-1$ line spectra is 50–70 mK for V892 Tau and HD 142666, 90–100 mK for HD 135344, HD 139614 and HD 179218 in 31 kHz channels (0.027 km s$^{-1}$). All sources, except V892 Tau, have been previously identified as isolated stars with no proximity to extended cloud material. We took two 30″ offset measurements, one to the east and the other to the south of V892 Tau and find that the line is dominated by extended cloud emission (See also Thi 2002). Figure 2 shows the spectra taken in the direction of the source and the offset positions. As a follow-up, the environment of V892 Tau is studied using HARP mapping towards V892 Tau (see Appendix for details).

The observations of the $^{12}$CO $J = 3-2$ line at 345.796 GHz towards HD 100546 were carried out using APEX on 2005 July 27, with an integration time of 15 minutes and the atmospheric opacity $\tau_{230\ \mathrm{GHz}} = 0.2$. The rms level obtained is 120 mK in 61 kHz channels (0.053 km s$^{-1}$). The APEX beam efficiency at 345 GHz is 0.73. This data will be presented fully in a forthcoming publication.

In this paper, we extensively use the $^{12}$CO $J = 3-2$ observations previously taken with the JCMT, and presented in Dent et al. (2005).

### 2.1. Gas and dust submillimetre emision towards the source sample

Table 1 lists our sources and their interferometric 1.3 mm fluxes from the literature. Considering the fact that the distance to the sources ranges from 84 pc for HD 135344 to 240 pc for HD 179218, the continuum measurements do not differ greatly from one source to another. Using the continuum fluxes, we obtain dust mass estimates for the discs in our sample, valid under assumption that the 1.3 mm emission is optically thin. To calculate the disc masses we assume the temperature of the discs to be in the range 30–40 K, as in the disc midplane for Herbig AeBe stars in the irradiated accretion disc models of D'Alessio et al. (2005) at 100–200 AU from the star. While the assumption of a single temperature introduces an error of 20–50% in our dust mass estimates, they are dominated by the highly uncertain dust millimetre emissivity in circumstellar discs. We adopt the dust emissivity at 1.3 mm of 2 cm$^2$ g$^{-1}$ (emissivity is expressed per gram of dust throughout the paper). The emissivity we adopt is at the high end of the range suggested by Draine (2006) and can be as low as 0.1 cm$^2$ g$^{-1}$, depending on the dust size and composition. Thus the estimates we provide can be considered as rough lower limits on dust mass.

The resulting dust masses are listed in Table 1 and are in the range of $0.4-6.9 \times 10^{-4}$ $M_\odot$. Adopting a gas-to-dust mass ratio $f_{\mathrm{g/d}} = 100$ this translates to total disc masses $M_{\mathrm{disc}} = M_{\mathrm{dust}}\ f_{\mathrm{g/d}}$ of roughly $10^{-3}-10^{-1}$ $M_\odot$, similar to the results of Beckwith et al. (1990) for discs around T Tauri stars.

The integrated intensities of the $^{12}$CO lines we observed are shown in brackets in Table 2 alongside the values taken from the literature (Dent et al. 2005; Raman et al. 2006; Panić et al. 2008; Isella et al. 2007; Piétu et al. 2005). We detect the $^{12}$CO $J = 2-1$ line from HD 142666, HD 139614, and V892 Tau, and the $^{12}$CO $J = 3-2$ line from HD 100546, but obtain only upper limits from $^{12}$CO $J = 2-1$ observations of HD 179218. Our observations towards HD 135344 are excluded from the analysis due to errors in data acquisition. The $^{12}$CO $J = 3-2$ integrated line intensities range from several to tenths of K km s$^{-1}$ as seen in Table 2 (except for HD 100546, the values are taken from

[1] This publication is based on data acquired with the Atacama Pathfinder Experiment (APEX). APEX is a collaboration between Max-Planck Institut für Radioastronomie, the European Southern Observatory, and the Onsala Space Observatory.

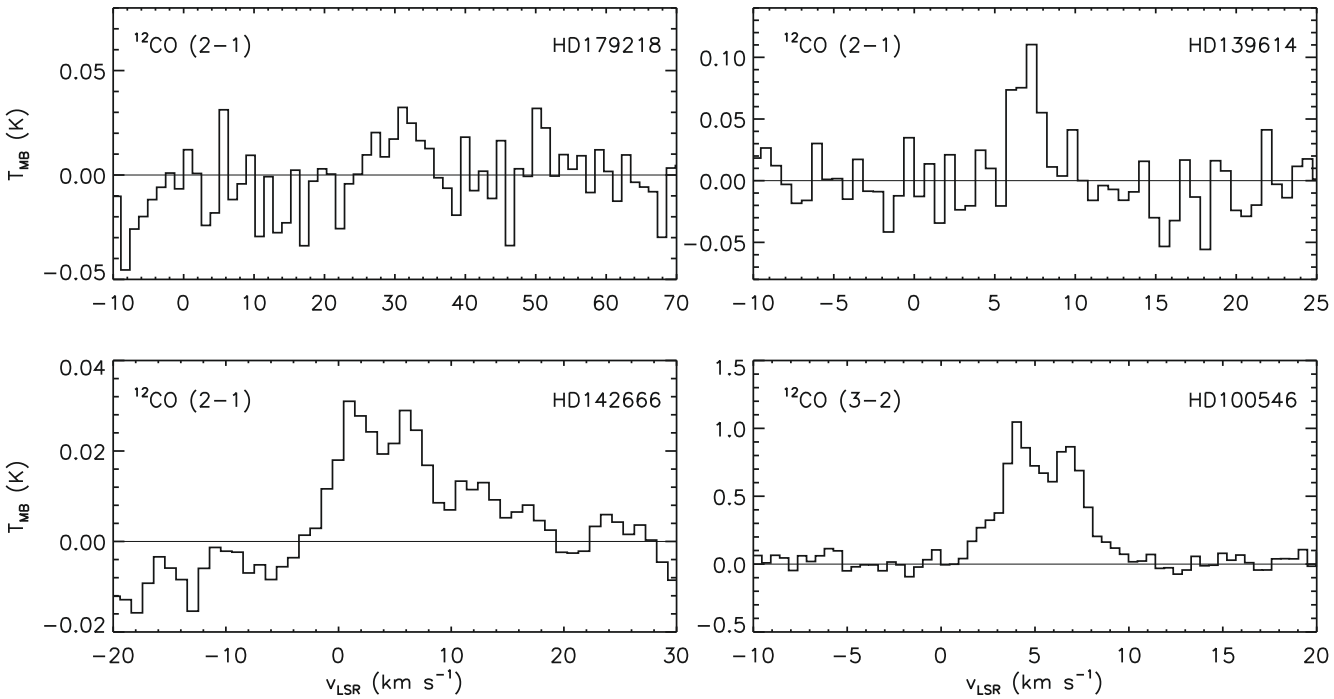


**Fig. 1.** Spectra of $^{12}$CO $J$ = 2−1 line observed towards HD 179218, HD 139614, and HD 142666 and $^{12}$CO $J$ = 3−2 line observed towards HD 100546.

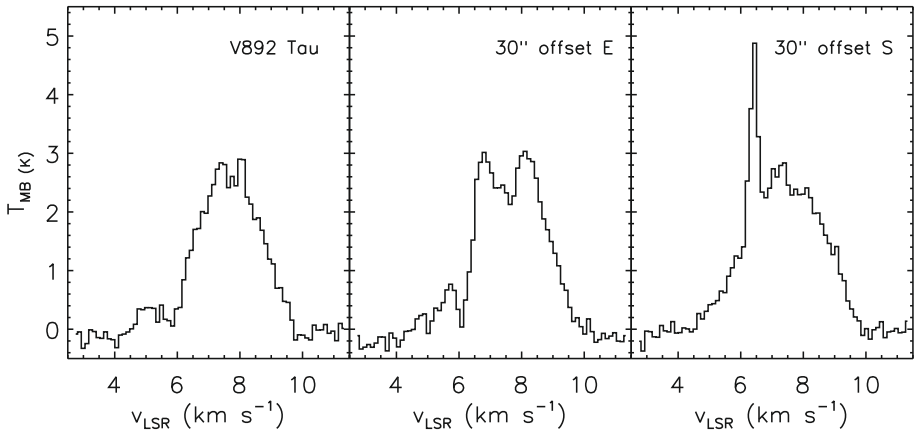


**Fig. 2.** Spectrum of the $^{12}$CO $J$ = 2−1 line observed towards V892 Tau and the two offset positions.

Dent et al. 2005). The strong sources HD 100546 and HD 163296 are also at the high end of estimated disc masses, while the weak sources HD 135344 and HD 142666 correspond to discs with masses close to $1 \times 10^{-2}$ $M_{\odot}$. The disc around AB Aur, in spite of the modest mass estimated from the dust continuum, shows the strongest $^{12}$CO $J$ = 3−2 line of 13.67 K km s$^{-1}$ (calculated from Thi et al. 2001). Some of this emission arises from the surrounding envelope (Nakajima & Golimowski 1995; Thi et al. 2001; Schreyer et al. 2008; Semenov et al. 2005).

For the $J$ = 3−2 and $J$ = 2−1 lines arising from the range of temperatures and densities typically found in discs, we expect similar intrinsic intensities (calculations done using the RADEX online tool, van der Tak et al. 2007). The ratio between the $^{12}$CO $J$ = 3−2 and $J$ = 2−1 integrated line intensities as observed with the JCMT is expected to be close to two. This ratio is dominated by the beam dilution, which scales with the square of the beam size. The observed integrated intensities of both lines are listed in Table 2, and their ratio shows that five of the sources are consistent with the expected ratio of two. One of the exceptions is V892 Tau, which shows excess $^{12}$CO $J$ = 2−1 line flux. This is due to the surrounding cloud material heavily contributing to the $^{12}$CO line emission in spatially unresolved single dish observations. The strong ambient emission around V892 Tau is confirmed in observations of the offset positions and mapping of the region with HARP (see Appendix for details). For this reason, we exclude V892 Tau from further analysis. The source HD 179218 has an upper limit on the $^{12}$CO $J$ = 2−1 line flux several times lower than the fluxes expected based on the $J$ = 3−2 line flux. This results in a large line ratio of 6, indicating that the $^{12}$CO $J$ = 3−2 emission toward this source is likely dominated by optically thin molecular gas at a higher temperature regime than found in discs (several hundreds Kelvin).

## 3. Comparison to the SED-based disc models

The SEDs of our sources were fitted by Dominik et al. (2003) using a disc structure based on the flaring passive disc model

**Table 1.** Stellar properties[a] and the derived dust mass of the discs.

| # | Source | Distance (pc) | Spectral type | Luminosity ($L_\odot$) | $M_{star}$ ($M_\odot$) | $F^c_{1.3\ mm}$ (mJy) | $T_{avg}$ (K) | $M_{dust}$ ($10^{-4}$ $M_\odot$) |
|---|---|---|---|---|---|---|---|---|
| (1) | HD 100546 | 103 | B9 | 36 | 2.5 | 470 | 30–40 | 2.1–2.9 |
| (2) | HD 179218 | 240 | B9 | 80 | 2.7 | 71 | 30–40 | 1.7–2.4 |
| (3) | V892 Tau[b] | – | B8 V | 400 | 5.5 | 230 | – | – |
| (4) | AB Aur | 144 | A0 | 47 | 2.5 | 100 | 30–40 | 0.9–1.2 |
| (5) | HD 163296 | 122 | A1–A3 | 30 | 2.4 | 780 | 30–40 | 4.9–6.9 |
| (6) | HD 169142 | 145 | A5 | 32 | 2.5 | 169[d] | 30–40 | 1.5–2.1 |
| (7) | HD 139614 | 157 | A7 | 12 | 1.8 | 240 | 30–40 | 2.5–3.5 |
| (8) | HD 142666 | 116 | A7–A8 | 11 | 1.8 | 127 | 30–40 | 0.7–1.0 |
| (9) | HD 135344 | 84 | F4–F8 | 3 | 1.3 | 140 | 30–40 | 0.4–0.6 |

[a] See Table 3 of Dominik et al. (2003), and references therein. [b] Binary system with two B8 V stars with total mass of 5.5 $M_\odot$ (Smith et al. 2005; Palla & Stahler 1993; Monnier et al. 2008). [c] Mannings & Sargent (1997), unless noted otherwise. [d] Raman et al. (2006).

**Table 2.** Observed $^{12}$CO $J = 3-2$ and $J = 2-1$ line integrated intensities and full width at half-maximum. Bracketted values are from this work. Calculated values for the $J = 3-2$ line, based on the SED-fitting disc model.

| Source | $\int I_{CO(3-2)}dV$ (K km s$^{-1}$) | $\int I_{CO(3-2)}{}^{calc}$ (K km s$^{-1}$) | $FWHM_{CO(3-2)}$ (km s$^{-1}$) | $FWHM\ ^{calc}_{CO(3-2)}$ (km s$^{-1}$) | $\int I_{CO(2-1)}dV$ (K km s$^{-1}$) | $(\int I_{CO(3-2)})/(\int I_{CO(2-1)})$ |
|---|---|---|---|---|---|---|
| HD 100546 | [5.96 ± 0.64] | 9.40 | [4.3] | 5.0 | – | – |
| HD 179218 | 0.60 ± 0.12 | 0.03 | 7.0 | 9.7 | [<0.11] | >6 |
| V892 Tau | [7.12 ± 0.20] | – | [1.6] | – | [8.23 ± 1.08] | 0.9 |
| AB Aur | 13.67 ± 1.6 | 4.73 | 1.4 | 5.7 | – | – |
| HD 163296 | 4.30 ± 0.10 | 0.33 | 4.0 | 16.2 | 2.94 | 1.5 |
| HD 169142 | 1.70 ± 0.13 | 0.31 | 1.6 | 2.3 | 0.91 | 1.9 |
| HD 139614 | 0.47 ± 0.11 | 0.12 | 2.0 | 6.3 | [0.30 ± 0.09] | 1.7 |
| HD 142666 | 0.72 ± 0.14 | 0.004 | 2.0 | 22.4 | [0.29 ± 0.06] | 2.4 |
| HD 135344 | 0.97 ± 0.04 | 9.84 | 1.8 | 4.4 | – | – |

**Table 3.** Disc outer radius and inclination ($i$=0 corresponds to the face-on orientation) as used in the SED fitting, from our parametric models, and direct observations.

| Source | SED modelling[a] | | | Parametric models ($p = 1$) | | Observed values | |
|---|---|---|---|---|---|---|---|
| | $R_{out}$ | $i$ | $p$ | $R_{out}$ | $i$ | $R_{out}$ | $i$ |
| HD 100546 | 400 | 51 | 0.0 | 300 | 45 | 350–380[b], 200[c] | 51 ± 3[b], 50 ± 5[c] |
| HD 179218 | 30 | 20 | –0.8 | 200 | 60 | – | – |
| AB Aur | 400 | 65 | 2.0 | >800 | 10–20 | 1050[d] | 33 ± 1[d] |
| HD 163296 | 50 | 65 | 0.2 | 350 | 40 | 540[e] | 46 ± 4[e] |
| HD 169142 | 100 | 8 | 2.0 | 200 | 5 | 235[f,g] | 13 ± 1[f,g] |
| HD 139614 | 60 | 20 | 0.1 | 100 | 0 | – | – |
| HD 142666 | 10 | 55 | –0.5 | 75 | 5 | – | – |
| HD 135344 | 800 | 60 | 0.8 | 50 | 5 | 210 [h], ≥150 [j] | 46 ± 5[h], 14 ± 4° [i], ≤20° [j] |

[a] Dominik et al. (2003) (note that they use $p$ as $\Sigma \propto R^p$). [b] Augereau et al. (2001), spatially resolved near-infrared coronographic scattered light observations. [c] Pantin et al. (2000), spatially resolved $J$ and $K$ band near-infrared observations. [d] Piétu et al. (2005), spatially resolved $^{12}$CO $J = 2-1$ line observations. [e] Isella et al. (2007), spatially resolved $^{12}$CO $J = 2-1$ and $J = 3-2$, and $^{13}$CO $J = 1-0$ line observations. [f] Raman et al. (2006), spatially resolved $^{12}$CO $J = 2-1$ line observations. [g] Panić et al. (2008), spatially resolved $^{12}$CO, $^{13}$CO and C$^{18}$O $J = 2-1$ line observations. [h] Doucet et al. (2006), mid-infrared interferometry. [i] Pontoppidan et al. (2008). [j] Grady et al. (2009).

of Chiang & Goldreich (1997). Modifications to the original Chiang & Goldreich (1997) models and the detailed disc parameters used in the fit can be found in Dominik et al. (2003) (see their Table 3) while our Table 3 lists the model parameters of direct relevance for the $^{12}$CO lines. The disc masses range from 0.01 to 0.1 $M_\odot$ and outer radii from 10 AU to 800 AU.

With the help of the molecular excitation and radiative transfer code RATRAN (Hogerheijde & van der Tak 2000), we calculate the $^{12}$CO $J = 2-1$ and $J = 3-2$ line emission from the SED disc models, assuming a standard gas-to-dust mass ratio of 100:1. In our calculations, we neglect the contribution of the hot disc surface layer because of the low density at the disc surface and efficient $^{12}$CO photodissociation. Therefore the disc is vertically isothermal and the temperature corresponds to the disc *midplane* temperature as used in Dominik et al. (2003). The disc temperature is well above the CO freeze-out temperature of 20 K in all the models except for the HD 135344 disc model beyond 400 AU from the star. For simplicity, we neglect any possible effect of freeze-out on the $^{12}$CO abundance in our analysis, and adopt a constant $^{12}$CO abundance of $10^{-4}$ with respect to $H_2$. The effect of microturbulence is included, with the equivalent linewidth of 0.16 km s$^{-1}$. Each calculated spectrum is convolved with the JCMT beam of the corresponding size, using the Miriad software package (Sault et al. 1995).

Columns 2 and 5 in Table 2 show the resulting integrated intensity and full width at half-maximum (*FWHM*) of the $^{12}$CO

**Table 4.** Model parameters.

| Parameter | Symbol | Type | Value(s) |
|---|---|---|---|
| Inclination | $i$ | variable | 0, 15, 30, 45, 60, 75, 90° |
| Outer radius | $R_{\rm out}$ | variable | 50, 10, 200, 400, 800 AU |
| Inner radius | $R_{\rm in}$ | fixed | 0.4 AU |
| Disc mass (gas+dust) | $M_{\rm disc}$ | fixed | 0.01 $M_\odot$ (test calculations also done, up to 0.07) |
| Surface density at 100 AU | $\Sigma_{100}$ | variable | calculated based on choice of $R_{\rm out}$ |
| Surface density exponent | $p$ | fixed | 1 |
| Temperature at 100 AU | $T_{100}$ | fixed | 30, 60 K |
| Temperature exponent | $q$ | fixed | 0.5 |
| Scale height at 100 AU | $h_{100}$ | fixed | $10^{12}$ m |
| Scale height exponent | $y$ | fixed | –1 |
| Turbulent equivalent line width | $dV$ | fixed | 0.16 km s$^{-1}$ |
| Stellar mass | $M_{\rm star}$ | fixed | 2.0 $M_\odot$ |
| Dust opacity | $\kappa$ | fixed | 2 cm$^2$g$^{-1}$ |

$J$ = 3–2 line. In comparison to the observed spectra, the modelled spectra of most sources underestimate the observed integrated intensities. This is especially pronounced for the discs with assumed outer radii of 10–50 AU, such as HD 142666, HD 179218 and HD 163296. The width of the modelled lines for HD 142666 and HD 163296 significantly exceeds the observations, supporting the argument for a larger outer radius than assumed in the SED modelling. The reason is that in a small disc, the material dominating the line emission rotates at relatively large velocities, and thus produces very wide spectral profiles, with *FWHM* roughly 10–20 km s$^{-1}$, while a large disc has a significant contribution from the slowly rotating material at large distances from the star. As mentioned, the SED is most sensitive to the region of a few tens of AU from the star. While the SED fitting is a valuable method to derive disc structure and temperature, when it is done without including the constraints on the disc size and inclination, the regions beyond 50 AU may not be accurately decribed. Some sources are modelled with a radially *increasing* surface density in Dominik et al. (2003). This was done to reproduce the slope of the mid-infrared emission at 10–30 $\mu$m wavelength, originating in the very inner disc regions, and is therefore not necessarily a good representation of the disc structure at larger scales as traced by the rotational $^{12}$CO lines. Recent work of Meijer et al. (2008) shows that the SED is almost insensitive to the disc outer radius, and this explains the almost systematic underestimate of disc outer radii in Dominik et al. (2003).

In the sources HD 135344 and HD 100546, with assumed radii of 800 and 400 AU respectively, the line emission is overestimated. A disc model with an outer radius closer to the observed 210 AU (Doucet et al. 2006) may provide a better fit to the $^{12}$CO $J$ = 3–2 line from HD 135344. In the model of HD 100546, a surface density exponent steeper than the assumed $p$ = 0 may provide a better fit to the observed $^{12}$CO line spectrum.

In the case of AB Aur, the relatively large assumed inclination of 65° is used to account for the relatively low near-infrared excess emission (Dominik et al. 2003). This choice of inclination is reflected in the larger *FWHM* of the modelled $^{12}$CO line than observed. However, the millimeter interferometry observations (Piétu et al. 2005) indicate an inclination of 33°, an outer radius of 1050 AU and an inner radius close to 50 AU. In sources like AB Aur, exhibiting a low near-infrared excess, it is thus essential to establish whether the apparent lack of near-infrared emission is due to a lack of material in the innermost disc regions (presence of an inner hole) or due to the large disc inclination. As seen in this example, the $^{12}$CO spectral line profile, as a diagnostic of disc inclination, provides a way to discriminate between these two scenarios, even in case of spatially unresolved, single dish observations. Meijer et al. (2008, their Fig. 2) show the strong dependence of the overall shape of the disc SED on the inclination, that stresses the necessity for reliable estimates of inclination.

## 4. Modelling and analysis of the $^{12}$CO $J$ = 3–2 spectra

In the previous section, we showed that the disc models based on the SED emission alone fail to simultaneously reproduce the observed spectral lines of CO. It is very useful to design a simple way to estimate the disc size and inclination from the observed $^{12}$CO spectra, providing valuable input into the SED modelling from the observational data already available for most gas-rich discs. In the current literature, the estimates of size and inclination are done predominantly through spectral line fitting with a large number of free model parameters. Here, we take a simpler approach.

The low-$J$ $^{12}$CO line emission is expected and often found to be optically thick in circumstellar discs. Therefore it traces a warm layer of gas above the disc midplane (van Zadelhoff et al. 2001; Dartois et al. 2003) and is relatively insensitive to the total disc mass. The emission is dominated by the disc material at scales of 100 AU from the star. For a known stellar mass, the shape of the line is sensitive to both disc size and inclination. In our approach, we focus on the parameters to which the presumably optically thick $^{12}$CO $J$ = 3–2 line is most sensitive: disc size, inclination and temperature, and make simple assumptions about the remaining parameters like the disc mass, inner radius, surface density exponent, and disc vertical temperature and density structure.

### 4.1. Power-law disc models

We develop a grid of simple parametric disc models to interpret the observed $^{12}$CO $J$ = 3–2 line profiles. Our models use a power-law surface density and temperature distribution: $\Sigma = \Sigma_{100}(R/100\,{\rm AU})^{-p}$ and $T = T_{100}(R/100\,{\rm AU})^{-q}$, and are comparable in the assumptions to those of Chiang & Goldreich (1997). The $^{12}$CO $J$ = 3–2 line is optically thick, with the optical depth $\tau \geq 10$ in our models. The line spectrum alone does not provide any insight into the vertical temperature structure of the disc. Thus we use a vertically isothermal disc structure and describe the line flux by an "effective" temperature representing a cummulative effect of the disc temperature structure on the line emission at the given radius. This simplification is

used in the analysis of the submillimetre $^{12}$CO emission in discs around T Tauri and Herbig Ae stars in the literature (Dutrey et al. 1994; Guilloteau & Dutrey 1998; Piétu et al. 2007, 2005; Isella et al. 2007). The vertical density structure is given by $n(z) = n_0 \exp(-z^2/2h^2)$ where $n_0 = \Sigma/\sqrt{\pi h}$ is the midplane density, and $h = h_{100}(R/100\,\mathrm{AU})$ is the scale height. The model parameters are listed in Table 4 along with the corresponding values.

We explore a wide range of *disc sizes*, with $R_{\rm out}$ from 50 to 800 AU, and the full range of *inclinations* with respect to the line of sight (0° corresponding to the face-on orientation). These are the two main parameters in our analysis. The parameters determining disc density structure ($p$, $M_{\rm disc}$) are held fixed, with values close to those observationaly derived in the literature for discs in general (Beckwith et al. 1990; Mannings & Sargent 1997). The disc mass is set to 0.01 $M_\odot$. While the optically thick low-$J$ $^{12}$CO lines are not very sensitive to the radial density distribution, their fluxes depend stongly on the temperature. We have two sets of calculations, one setting the temperature at 100 AU to $T_{100} = 30$ K and the other for $T_{100} = 60$ K. We adopt the slope $q = 0.5$ for the temperature radial dependence, as found to describe the $^{12}$CO emission well in a number of sources (Thi et al. 2001; Piétu et al. 2007). In a more realistic modelling, $T_{100}$ could be anywhere in this approximate range, depending on the exact spectral type, disc geometry, dust settling and other properties of each source. Below we argue that $T_{100} = 60$ K, close to the values derived in the parametric modelling of the interferometric observations of the $^{12}$CO $J = 2{-}1$ line in AB Aur and MWC 480 (Piétu et al. 2007, 2005), provides a better fit to the disc size for several objects where we have independent measurements of the outer radius, and describes the observed line spectra from Dent et al. (2005) well.

The velocity field is given by Keplerian rotation around a central star with a mass of $M_{\rm star} = 2.0\,M_\odot$. This value describes our sample of sources (Table 1) well, considering the spectral resolution of the data, and that the line width depends on $\sqrt{M_{\rm star}}$. Turbulent line broadening is included, with the equivalent line width of 0.16 km s$^{-1}$. Its influence on the results of our simple analysis is negligible. The calculations of the synthetic spectra are done using RATRAN. The $^{12}$CO abundance is set to a constant value of $10^{-4}$ throughout the disc. Dust is included in the radiative transfer calculation of the $^{12}$CO $J = 3{-}2$ line, adopting a gas-to-dust mass ratio of 100:1 and with a dust submillimetre emissivity of 2 cm$^2$g$^{-1}$. All calculations were done with an adopted distance of 140 pc. We will later scale the observations to the same distance. The calculated spectra were convolved with the 14″ beam of the JCMT and the contribution of the dust continuum to the integrated line intensity was subtracted. We compare the calculated *FWHM* and $\int I\mathrm{d}V$ with the observed *FWHM* and $\int I\mathrm{d}V \times (d/140\,\mathrm{pc})^2$, where $d$ is the actual distance of the source.

### 4.2. Model results

The results from our grid of models with $T_{100} = 60$ K are presented in Fig. 3a, where the line integrated intensity is plotted against the *FWHM*. The full lines connect varying inclinations at constant radius, while the dotted and dashed lines connect model results at varying radii for a fixed inclination. The two parameters, disc size and inclination, are non-degenerate at inclinations 0°–45°. In this range, the *FWHM* grows with the inclination, and the integrated line intensity with the size of the disc. For a fixed $R_{\rm out}$, at inclinations larger than 60° the line integrated intensity drops sharply, at an almost constant *FWHM* in larger discs towards the results corresponding to a smaller disc with a slightly lower inclination. At very high inclinations, the emission in the line wings is relatively unaffected by the exact value of the inclination. However, the line emission between the two peaks in the spectrum that dominates the line intensity at $i < 45°$ decreases as the inclination increases beyond this value. This is because the contribution from the warm disc layers is gradually absorbed by the superposed outermost disc regions of low temperature that begin to dominate the line emission as the inclination increases from 45° to 90°. Therefore, at high inclinations the parameters $i$ and $R_{\rm out}$ become degenerate, and the spectra cannot be fitted by a single model in the region to the right of the $i = 45°$ curve in Fig. 3a.

For comparison, the observed *FWHM* and $\int I\mathrm{d}V \times (d/140\,\mathrm{pc})^2$ values are plotted in Fig. 3 (triangles) for 21 Herbig Ae/Be discs from Dent et al. (2005) and our source HD 100546. The integrated intensities are scaled to the 140 pc distance using the distances given in the same paper (except for HD 34282, where we adopt 160 pc as in van den Ancker et al. (1998). All sources fall within the span of our model results, while several very weak sources appear to require a radius smaller than our smallest size of 50 AU. Our model results are roughly consistent with some of the known disc radii and inclinations (AB Aur, HD 169142, HD 163296), determined through millimetre interferometry. Table 3 lists the disc outer radii and inclinations derived from the SED modelling alongside the values we find from our parametric disc models. For some of the sources, sizes and inclinations measured directly via near-infrared and/or submillimetre imaging are also listed, for comparison. In the following section we discuss the implications of the model fit for each of our sources in detail.

Close to 75% of the sources, or 17 out of the 22 sources, from Dent et al. (2005) have integrated line intensity lower than 2 K km s$^{-1}$, when scaled to 140 pc distance. In terms of our modelling this translates to sizes smaller than 200 AU, a result consistent with the disc size estimates in Dent et al. (2005, their Table 2). The disc size is very sensitive to the assumed $T_{100}$. However, while the optimal value of $T_{100}$ may vary from one source to another depending on the exact spectral type of the star and disc geometry, $T_{100} = 60$ K appears to represent our sample of the discs aroud Herbig AeBe stars well. In the light of this result, the sources with large outer radii like AB Aur, MWC480 and HD 163296, studied extensively with the sub-millimetre interferometers, have disc structures that are not necessarily a good representation of the entire sample of discs around intermediate mass stars. The smaller discs, although observationally more challenging, may hold clues to the processes that shape discs in the course of their evolution. Furthermore, their small size, coupled with the illumination by an A-type star, provides a fair chance that the CO depletion is not significant, leading to a better gas mass estimate than can be done in discs around T Tauri stars. The structure of some of these discs, close to 200 AU in size, has already been studied (Chapillon et al. 2008; Panić et al. 2008). Spatially resolved observations of more sources would also provide an answer to how many of these *weaker* sources are indeed small versus those that are perhaps larger but have lost a significant mass fraction of their gas or have cleared a large inner hole.

Figure 3b shows the results for models with $T_{100} = 30$ K. In comparison with the set of models with a higher temperature it is clear that the line strength, i.e., $\int I\mathrm{d}V$ decreases with temperature. In this sense, $R_{\rm out}$ and $T_{100}$ are degenerate parameters.

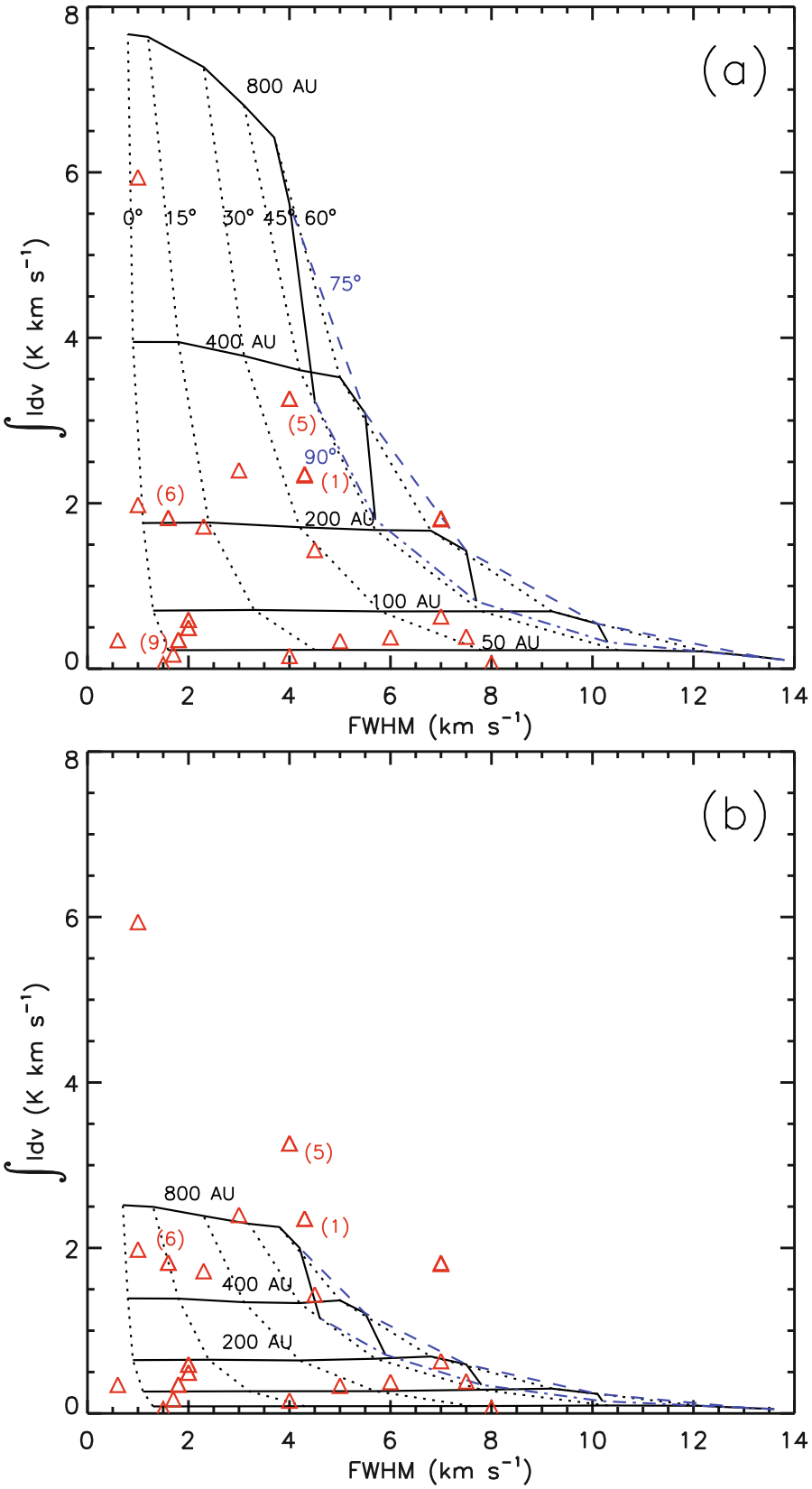


**Fig. 3.** Integrated intensity of the modelled $^{12}$CO $J$ = 3–2 line emission, plotted versus the *FWHM*, for $M_{\rm star}$ = 2.0 $M_\odot$ and $M_{\rm disc}$ = 0.01 $M_\odot$. The panels **a)** and **b)** show the results of the parametric disc models with $T_{100}$ = 60 K and 30 K, respectively. The full black lines connect the results of models at a constant disc outer radius, the value of which is labeled. The dotted black and dashed blue lines connect the results for a constant inclination, also labeled. The triangles are the observed values, from Dent et al. (2005) and this work, with the observed integrated line intensities scaled as $\int I{\rm d}V \times (d/140\,{\rm pc})^2$. Some of the sources from Table 1 are labeled by number.

The models with $T_{100}$ = 30 K fail to describe the observed integrated line intensity and *FWHM* of a number of sources, mainly the ones with $\int I{\rm d}V \times (d/140\,{\rm pc})^2 > 2$ K km s$^{-1}$ and *FWHM* > 4 km s$^{-1}$. The only way for this group of models to reproduce all observations would be to adopt very large disc sizes, e.g., $R_{\rm out} \approx 600$ AU for HD 169142, and higher stellar masses, e.g., $M_{\rm star} \approx 5\,M_\odot$ for HD 179218, both significantly larger than the values observed in some of our sources. Therefore, a higher temperature of $T_{100} \approx 60$ K appears to be a good choice for the sample.

Our parametric disc models are designed to reproduce the low-$J$ $^{12}$CO line emission, and therefore they provide a description of the disc structure at large scales, where most of this emission arises. These regions dominate the dust thermal continuum emission at long wavelengths (>300 $\mu$m), but the large uncertainties in the dust (sub)millimetre emissivity that heavily affects the continuum flux do not allow us to test the disc structure we derive against the observed SEDs. For an opportune choice of the dust emissivity within the wide range expected in discs (Draine 2006), our disc models provide submillimetre SED slopes consistent with those observed.

### 4.3. Individual sources

Here, we compare the results of our model with $T_{100}$ = 60 K to the SED modelling results and results from spatially resolved observations, where available. The comparison among the derived disc sizes and inclinations is shown in Table 3. The precise estimate of these two parameters requires spatially resolved observations, therefore the estimates from single dish observations must be considered as rough indications rather than measurements.

#### 4.3.1. HD 100546

The $^{12}$CO 3–2 emission is well described by our model with $R_{\rm out}$ = 300 AU, not too different from the 400 AU used in the SED model. The difference in size can account for the factor of two overestimate of the observed line emission by the SED model. Our inclination of 35° is somewhat lower than the 51 ± 3° observed with NICMOS scattered light imaging (Augereau et al. 2001) and used by Dominik et al. (2003) in their modelling, but is consistent with these values. Within the uncertainties involved in our model, our estimate of 300 AU is close to the 350–380 AU reported by Augereau et al. (2001). Spatially resolved $J$ and $K$ band near-infrared observations using the ADONIS instrument indicate an inclination of 50 ± 5° and a somewhat smaller size of 200 AU (Pantin et al. 2000), that can be considered as a lower limit to the actual disc radius.

#### 4.3.2. HD 179218

There are no direct measurements of the disc size and inclination in the literature. In Sect. 2.1 we mention that the $^{12}$CO $J$ = 3–2 line perhaps does not arise from the disc but is dominated by optically thin gas at a very high temperature. If we assume that the emission does arise from the disc, we derive the disc radius of 200 AU and the inclination of 60–75°. A larger disc size, up to 400 AU with an inclination of 75° is also possible. Our estimates of $R_{\rm out}$ are much larger than the radius of 30 AU used in the SED modelling.

#### 4.3.3. AB Aur

Our estimate of $R_{\rm out}$ > 800 AU and $i$ = 10–20° for AB Aur disc is reasonably close to the 1050 ± 10 AU and 33 ± 1° derived by Piétu et al. (2005) from the spatially resolved observations of the $^{12}$CO 2–1 line in this disc. The overestimate of the inclination in the SED fit would be avoided if the inner hole, estimated by Piétu et al. (2005) to be 45 ± 3 AU large in this disc, is included.

#### 4.3.4. HD 163296

We obtain a size of 350 AU, roughly consistent with the observationally derived 540 AU in Isella et al. (2007), via spatially resolved sub-millimetre observations. Our inclination of 40° is close to the 46 ± 4° derived therein. The disc size of 50 AU used in the SED modelling is much smaller.

#### 4.3.5. HD 169142

The disc size and inclination from SED modelling, our parametric models, and spatially resolved observations are all close. In Raman et al. (2006) the disc around HD 169142 was studied with spatially resolved $^{12}$CO 2–1 line emission, indicating a disc radius of 235 AU and inclination of 13°. Panić et al. (2008) find that an SED model described in Dent et al. (2006) and Raman et al. (2006) provides a good descripton of the $^{12}$CO and isotopologue line emission. Dominik et al. (2003) use a somewhat smaller disc size of 100 AU, while an extension of their model to 200 AU and perhaps with a less steep density exponent $p$ would probably be sufficient to reproduce the $^{12}$CO line emission.

#### 4.3.6. HD 139614

The SED modelling produces a weak and broad line, while a nearly face-on orientation is required to reproduce the observed narrow 3–2 line of $^{12}$CO towards HD 139614 (Dent et al. 2005). Our model fit results in $R_{\rm out}$ = 75−100 AU and $i$ = 5°, consistent with 110 AU and $i$ < 10° found by Dent et al. (2005), while the SED model has a slightly smaller disc size of 50 AU. Although there are no direct imaging measurements of the size of the disc around HD 139614, the weak $^{12}$CO lines would be very difficult to reproduce by a disc much larger than 100 AU unless the disc is colder, or has a very low gas (or CO) mass. The continuum flux of this source (Table 1) does not seem to indicate a very low disc mass (0.035 $M_\odot$), however.

#### 4.3.7. HD 142666

To reproduce the observed narrow $^{12}$CO line, an outer radius much larger than the 10 AU assumed in the SED modelling is needed, as well as a much lower disc inclination. We obtain a 75 AU radius and a 5° inclination for this disc. There are no direct measurements of these parameters for HD 142666 in the literature, however.

#### 4.3.8. HD 135344

Our derived disc size of 50 AU and an almost face-on orientation of 5° are consistent with the 14 ± 4° derived from spectroastrometric imaging with CRIRES (Pontoppidan et al. 2008), but in contradiction with the 210 AU outer radius and 46 ± 5° inclination observed using MIDI instrument (Doucet et al. 2006). The 1.3 mm continuum flux leads to a disc mass estimate of 0.01 $M_\odot$ (Sect. 2.1). A model with this disc mass, a 210 AU radius and 46° inclination would have a roughly three times stronger and wider $^{12}$CO 3–2 line than observed. At 8 ± 4 Myr, it is possible that this disc has lost significant amounts of its gas, but this does not explain the narrow line width. A presence of a considerably large inner hole, as indicated by the disc SED Brown et al. (2007), would remove the contribution of rapidly rotating material from the inner disc regions in the line profile and allow a narrow $^{12}$CO line to arise from a disc at 46 ± 5° inclination. If the process that caused the inner hole also helped to remove

or dissociate most of CO gas in the outer disc regions while not affecting the dust (e.g., photoevaporation), we may have a weak and narrow $^{12}$CO line profile from the disc described by 210 AU size and 46° inclination as observed with MIDI.

## 5. Conclusions

In this paper, we analyse the low-$J$ $^{12}$CO spectral lines and the dependence of their profiles on disc parameters, in particular the size and inclination. We present simple parametric disc models and find that the low-$J$ $^{12}$CO spectral line profiles are a valuable indicator of disc inclination and size, even in spatially unresolved observations.

We place our analysis in the context of the disc structure derived based on the SED modelling. We conclude that the "outside-in" disc modelling, i.e., starting from submillimetre $^{12}$CO spectral line observations or direct imaging of the dust thermal or scattered light emission, followed by the overall SED fitting, is more straightforward and provides more reliable results than the standard "inside-out" disc modelling where the SED is fitted with no prior knowledge of disc size and inclination and subsequently the outer disc emission interpreted in the context of the SED fitting results. The "outside-in" modelling of the disc structure helps remove degeneracies between disc inner radius and inclination, and provides a better estimate of the disc mass. For this purpose, we have developed a simple tool to get a rough indication of disc size and inclination for discs around Herbig Ae/Be stars from the observed $J = 3-2$ $^{12}$CO spectral line profiles.

We find that the great majority (75%) of observed discs around Herbig Ae/Be stars have sizes smaller than 200 AU, while discs much larger than 200 AU (e.g., AB Aur) are rare and not representative of the whole sample. We stress the importance of studying the gas content of the small discs, facilitated by the fact that they are typically warmer and allow us to minimise or even overcome the problem of CO depletion. Some of the weaker sources may be large and gas-poor discs, and it would be particularly interesting to spatially resolve these discs through millimetre continuum observations. If the weak sources are mainly the large and gas-poor discs, this would strengthen the conclusions about disc structure already derived from observations of bright sources. If, on the other hand, the vast majority of the weak sources are confirmed to be gas-rich discs small in size in spatially resolved observations, these will be perfect targets for measuring gas masses and ultimately the gas-to-dust mass ratio. Due to the sufficiently strong millimetre fluxes, the existing submillimetre interferometers can be used to derive disc sizes and measure gas mass of 200 AU large gas-rich discs. The high sensitivity and spatial resolution that ALMA will provide in the coming years will enable us to explore the weaker sources and the detailed structure of small discs.

## Appendix A: HARP mapping of the V892 Tau region

Following the detection of $^{12}$CO $J = 2-1$ line emission at the offset positions from V892 Tau, we mapped this region using the 16-pixel heterodyne array receiver HARP-B on the JCMT. The observations were carried out on 2008 September 10. The line observed was $^{12}$CO $J = 3-2$ at 345.796 GHz, with the beam size of 14″ and beam efficiency of 0.73. The rms obtained is 0.13 K per channel, at the spectral resolution of 0.026 km s$^{-1}$. The receiver array provided 11 spectra taken on a 4 × 4 raster, with the separation of 30″. The resulting spectra are shown in

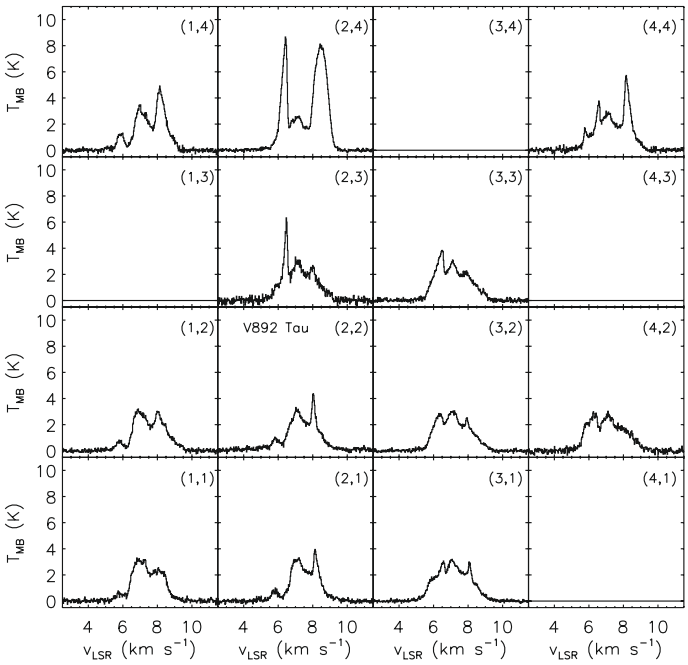


**Fig. A.1.** HARP mapping of the V892 Tau region. The spectrum toward V892 Tau is marked.

Fig. A.1. The spectrum taken at the (2, 2) position corresponds to the source V892 Tau. The integrated line emission is 7.12 ± 0.20 K km s$^{-1}$ and $FWHM$ = 1.6 km s$^{-1}$. These data show that V892 Tau is located in a region where the low-$J$ $^{12}$CO lines are dominated by the extended cloud material.

*Acknowledgements.* The research of O.P. and M.R.H. is supported through a VIDI grant from the Netherlands Organisation for Scientific Research. We are grateful to C. Dominik for providing us with the SED models and useful comments, and to W.-F. Thi for providing some additional data. We thank D. M. Salter and R.P.J. Tilanus for their technical support prior to, and during the JCMT observations.

## References

Augereau, J. C., Lagrange, A. M., Mouillet, D., & Ménard, F. 2001, A&A, 365, 78
Beckwith, S. V. W., Sargent, A. I., Chini, R. S., & Guesten, R. 1990, AJ, 99, 924
Bouwman, J., Meeus, G., de Koter, A., et al. 2001, A&A, 375, 950
Brown, J. M., Blake, G. A., Dullemond, C. P., et al. 2007, ApJ, 664, L107
Chapillon, E., Guilloteau, S., Dutrey, A., & Piétu, V. 2008, A&A, 488, 565
Chiang, E. I., & Goldreich, P. 1997, ApJ, 490, 368
D'Alessio, P., Merín, B., Calvet, N., Hartmann, L., & Montesinos, B. 2005, Rev. Mex. Astron. Astrofis., 41, 61
Dartois, E., Dutrey, A., & Guilloteau, S. 2003, A&A, 399, 773
Dent, W. R. F., Greaves, J. S., & Coulson, I. M. 2005, MNRAS, 359, 663
Dent, W. R. F., Torrelles, J. M., Osorio, M., Calvet, N., & Anglada, G. 2006, MNRAS, 365, 1283
Dominik, C., Dullemond, C. P., Waters, L. B. F. M., & Walch, S. 2003, A&A, 398, 607
Doucet, C., Pantin, E., Lagage, P. O., & Dullemond, C. P. 2006, A&A, 460, 117
Draine, B. T. 2006, ApJ, 636, 1114
Dullemond, C. P., & Dominik, C. 2004, A&A, 417, 159
Dullemond, C. P., & Dominik, C. 2005, A&A, 434, 971
Dutrey, A., Guilloteau, S., & Simon, M. 1994, A&A, 286, 149
Grady, C. A., Schneider, G., Sitko, M. L., et al. 2009, ApJ, 699, 1822
Guilloteau, S., & Dutrey, A. 1994, A&A, 291, L23
Guilloteau, S., & Dutrey, A. 1998, A&A, 339, 467
Hogerheijde, M. R., & van der Tak, F. F. S. 2000, A&A, 362, 697
Isella, A., Testi, L., Natta, A., et al. 2007, A&A, 469, 213
Malfait, K., Bogaert, E., & Waelkens, C. 1998, A&A, 331, 211
Mannings, V., & Sargent, A. I. 1997, ApJ, 490, 792
Mannings, V., & Sargent, A. I. 2000, ApJ, 529, 391
Meijer, J., Dominik, C., de Koter, A., et al. 2008, A&A, 492, 451
Monnier, J. D., Tannirkulam, A., Tuthill, P. G., et al. 2008, ApJ, 681, L97

Nakajima, T., & Golimowski, D. A. 1995, AJ, 109, 1181
Natta, A., Grinin, V., & Mannings, V. 2000, Protostars and Planets IV, 559
Palla, F., & Stahler, S. W. 1993, ApJ, 418, 414
Panić, O., Hogerheijde, M. R., Wilner, D., & Qi, C. 2008, A&A, 491, 219
Pantin, E., Waelkens, C., & Lagage, P. O. 2000, A&A, 361, L9
Piétu, V., Guilloteau, S., & Dutrey, A. 2005, A&A, 443, 945
Piétu, V., Dutrey, A., & Guilloteau, S. 2007, A&A, 467, 163
Pinte, C., Padgett, D. L., Ménard, F., et al. 2008, A&A, 489, 633
Pontoppidan, K. M., Blake, G. A., van Dishoeck, E. F., et al. 2008, ApJ, 684, 1323
Raman, A., Lisanti, M., Wilner, D. J., Qi, C., & Hogerheijde, M. 2006, AJ, 131, 2290
Sault, R. J., Teuben, P. J., & Wright, M. C. H. 1995, in Astronomical Data Analysis Software and Systems IV, ed. R. A. Shaw, H. E. Payne, & J. J. E. Hayes, ASP Conf. Ser., 77, 433
Schreyer, K., Guilloteau, S., Semenov, D., et al. 2008, A&A, 491, 821
Semenov, D., Pavlyuchenkov, Y., Schreyer, K., et al. 2005, ApJ, 621, 853
Smith, K. W., Balega, Y. Y., Duschl, W. J., et al. 2005, A&A, 431, 307
Tannirkulam, A., Monnier, J. D., Harries, T. J., et al. 2008, ApJ, 689, 513
Thi, W.-F. 2002, Ph.D. Thesis, Leiden University, February 2002
Thi, W. F., van Dishoeck, E. F., Blake, G. A., et al. 2001, ApJ, 561, 1074
Thi, W.-F., van Zadelhoff, G.-J., & van Dishoeck, E. F. 2004, A&A, 425, 955
van Boekel, R., Waters, L. B. F. M., Dominik, C., et al. 2003, A&A, 400, L21
van den Ancker, M. E., de Winter, D., & Tjin A Djie, H. R. E. 1998, A&A, 330, 145
van der Tak, F. F. S., Black, J. H., Schöier, F. L., Jansen, D. J., & van Dishoeck, E. F. 2007, A&A, 468, 627
van Zadelhoff, G.-J., van Dishoeck, E. F., Thi, W.-F., & Blake, G. A. 2001, A&A, 377, 566